



ELSEVIER

Available online at [www.sciencedirect.com](http://www.sciencedirect.com)

ScienceDirect

[www.elsevier.com/locate/jes](http://www.elsevier.com/locate/jes)

JES

JOURNAL OF  
ENVIRONMENTAL  
SCIENCES[www.jesc.ac.cn](http://www.jesc.ac.cn)

# Effects of meteorological conditions and topography on the bioaccumulation of PAHs and metal elements by native lichen (*Xanthoria parietina*)

Julien Dron<sup>1,\*</sup>, Aude Ratier<sup>1,4</sup>, Annabelle Austruy<sup>1</sup>, Gautier Revenko<sup>1</sup>,  
Florence Chaspoul<sup>2</sup>, Emmanuel Wafo<sup>3</sup>

<sup>1</sup>Institut Écocitoyen pour la Connaissance des Pollutions, Fos-sur-Mer, France

<sup>2</sup>Aix Marseille Université, Avignon Université, CNRS UMR-7263, IRD-237, IMBE, Marseille, France

<sup>3</sup>Aix Marseille Université, INSERM U-1261, SSA, IRBA, MCT, Marseille, France

<sup>4</sup>Université de Lyon, Université Lyon 1, CNRS UMR-5558, LBBE, Villeurbanne, France

## ARTICLE INFO

### Article history:

Received 12 November 2020

Revised 30 March 2021

Accepted 30 March 2021

### Keywords:

Indigenous lichen

Biomonitoring

Climate

Seasonal impacts

Sampling uncertainties

Integration time

## ABSTRACT

The bioaccumulation of PAHs and metal elements in the indigenous lichens *Xanthoria parietina* was monitored during two years at a quarterly frequency, in 3 sites of contrasted anthropic influence. The impact of the meteorological factors (temperature, relative humidity, rainfall, wind speed) was first estimated through principal component analysis, and then by stepwise multilinear regressions to include wind directions. The pollutants levels reflected the proximity of atmospheric emissions, in particular from a large industrial harbor. High humidity and mild temperatures, and in a lower extent low wind speed and rainfall, also favored higher concentration levels. The contributions of these meteorological aspects became minor when including wind direction, especially when approaching major emission sources. The bioaccumulation integration time towards meteorological variations was on a seasonal basis (1–2 months) but the wind direction and thus local emissions also relied on a longer time scale (12 months). This showed that the contribution of meteorological conditions may be prevalent in remote places, while secondary in polluted areas, and should be definitely taken into account regarding long-term lichen biomonitoring and inter-annual comparisons. In the same time, a quadruple sampling in each site revealed a high homogeneity among supporting tree species and topography. The resulting uncertainty, including sampling, preparation and analysis was below 30% when comfortable analytical conditions were achieved. Finally, the occurrence of unexpected events such as a major forest fire, permitted to evaluate that this type of short, although intense, events did not have a strong influence on PAH and metals bioaccumulation by lichen.

© 2021 The Research Center for Eco-Environmental Sciences, Chinese Academy of Sciences. Published by Elsevier B.V.

\* Corresponding author.

E-mail: [julien.dron@institut-ecocitoyen.fr](mailto:julien.dron@institut-ecocitoyen.fr) (J. Dron).

## Introduction

The estimation of atmospheric contamination by metal elements and polycyclic aromatic hydrocarbons (PAHs) measured through their bioaccumulation in lichen has been employed since decades (Nieboer et al., 1972; Carlberg et al., 1983; Bargagli et al., 1987), and has since considerably expanded worldwide. Among other, recent works focused on compounds of emerging interest (Zhu et al., 2015; Vannini et al., 2016; Dauphin et al., 2020), improving interpretation scales (Cecconi et al., 2019), or new features such as evaluating the contributions of pollution sources (Boamponsem et al., 2017; Ratier et al., 2018; Contardo et al., 2020; Dörter et al., 2020). Biomonitoring with lichens benefits from major structural and physiological qualities. These symbiotic organisms remain active all year round and several species are widely distributed in many types of environments including polluted areas, allowing sampling campaigns to take place nearly anywhere and at any time. By the lack of protective cuticle and root system as well as a large specific area, lichens are essentially dependent of atmospheric inputs, and the accumulation of contaminants in lichens is considered as representative of air concentrations (Nimis et al., 2002).

Recent research also targeted the mechanisms involved in contaminants bioaccumulation (Augusto et al., 2015; Paoli et al., 2018a), the influence of environmental (e.g. climate, topography...) and physiological factors (Godinho et al., 2009; Capozzi et al., 2020; Rola et al., 2020), and the integration time for lichens to accumulate atmospheric contaminants (Godinho et al., 2008; Paoli et al., 2018b; Zhao et al., 2019). Most of these studies show that these parameters can constitute an important source of variability. A large majority cannot, or only partially, be managed by the field sampling strategy, among which physiological aspects, site characteristics such as local topography and supporting tree species, and climatic conditions. These issues still require an improved knowledge to precise how the measurements are representative of the atmospheric contaminants levels and to refine the appropriate conditions and methodologies that should be considered according to the study purpose (Adams and Gottardo, 2012; Paoli et al., 2018a, 2018b; Fortuna and Tretiach, 2018).

Seasons and climatic conditions can have an influence on atmospheric particulate pollution in Mediterranean regions (Salameh et al., 2015; Alves et al., 2017), and also likely impact the lichen bioaccumulation levels. In Southern Europe, while lower temperatures and higher humidity were found to improve the vitality and the growth rate of lichen (Vieira et al., 2017; Fortuna and Tretiach, 2018), studies focusing on metal elements bioaccumulation in lichen showed that the incidence of rainfall was minor (Bergamaschi et al., 2007) and that no difference occurred between summer and winter seasons (Malaspina et al., 2014). On the other hand, a significant seasonal effect was shown towards PAH levels in lichen transplanted to polluted environments, suggesting a prominent incidence of biomass burning in winter (Kodnik et al., 2015; Capozzi et al., 2020).

Many of these works were carried out with transplanted individuals, while native lichen was rarely surveyed among

long periods of time on the same sites. However, both transplant and native lichen biomonitoring techniques present inherent qualities and limits, and are widely employed by research teams as well as environmental consulting companies. In this study, we aim at improving the knowledge of the bioaccumulation phenomenology of native lichen, and thus, its biomonitoring methodology. Therefore, we have investigated the bioaccumulation patterns of indigenous *Xanthoria parietina* in three sites of contrasted anthropic influences, by quarterly samplings during two years. Statistical analyses were performed to identify the climatic parameters and conditions that have an influence on the bioaccumulation of PAHs and metals in lichen thalli. In relation with the seasonal and atmospheric aspects of air pollution, as well as with the physiological activity of the lichen, the climatic conditions may have a short or long-term impact on the contaminant bioaccumulation. This aspect is not well documented at this time, in particular for native lichen (Fortuna and Tretiach, 2018; Zhao et al., 2019), and thanks to the regular samplings performed here, it was included in the present statistical work. Moreover, the sampling uncertainty, as well as the incidence of short but potentially impacting events (forest fire, construction works) are discussed.

## 1. Materials and methods

### 1.1. Site description

The sampling area (Fig. 1), fully described in Ratier et al. (2018), is located in Fos-sur-Mer by the greatest maritime industrial area in France. The site numbering has been conserved from Ratier et al. (2018), with the “u” and “i” letters referring to urban and industrial environments, respectively. The sites were chosen by considering their contrasted environments regarding the study of seasonal variations. Thus, site “u3” is located in the Grans town (population approx. 5000) away from industries but potentially impacted by regional influences, local biomass burning emissions (agricultural, heating), and road traffic from the nearby city of Salon-de-Provence (population approx. 45,000) and highway node; site “i5” lies under industrial influence away from urban centers; site “ui1” is located in Port-Saint-Louis-du-Rhône (population approx. 9000) and may be particularly subjected to both biomass burning and industrial emissions (Fig. 1, Ratier et al., 2018).

### 1.2. Meteorology

The meteorological data (temperature TC, rainfall RR, relative humidity RH, wind speed WS and wind direction WD) originate from the Meteo-France station of Istres, which has a central position towards the lichen collection sites, being about 7 km from the site i5 and 15 km from ui1 and u3 (Fig. 1).

The local climate is typically Mediterranean, benefiting from a hot and dry summer with very little rainfall from May to August, and a mild winter with daily mean temperatures above 5 °C. The evolution of the meteorological parameters during the 2 years of the quarterly samplings is presented in Fig. 1. It can also be noticed from the annual wind roses that northwesterly winds are dominating (48% of the studied pe-

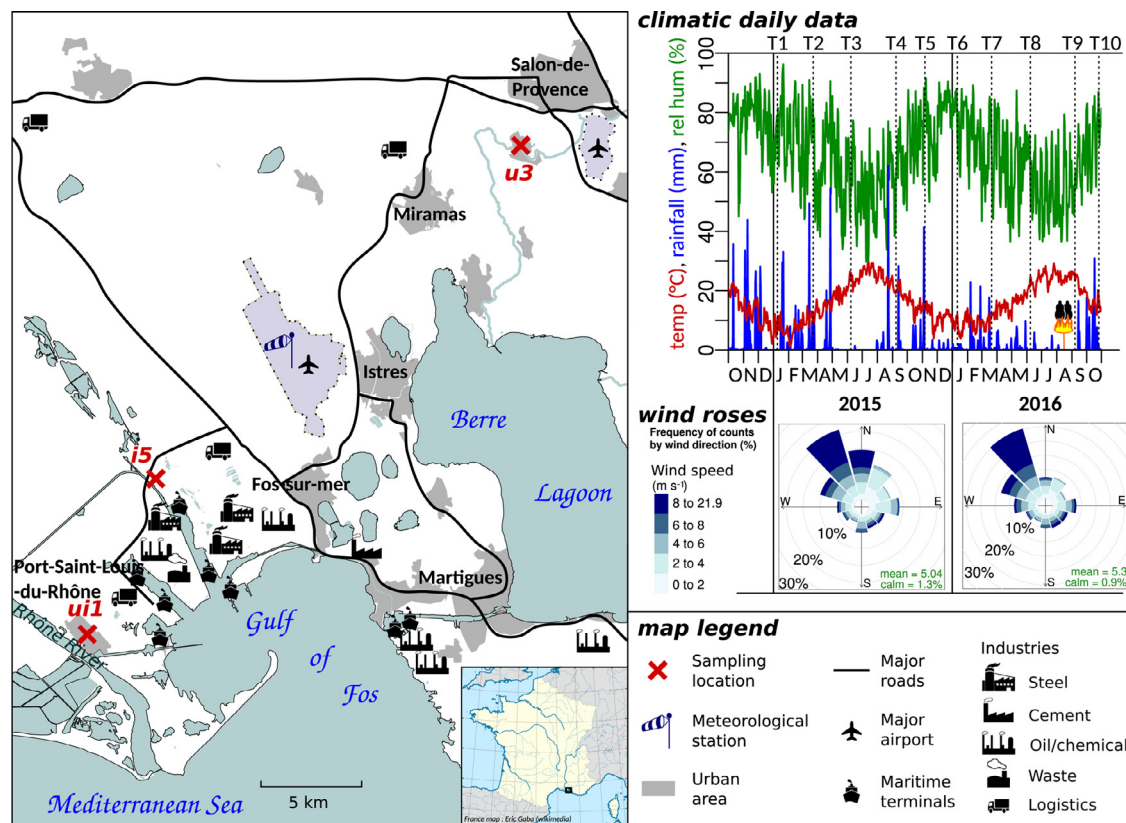


**Fig. 1** – Location of the study sites and meteorological conditions during the two-year sampling period. The fire pictogram in the climatic daily data represents a 711 Ha forest fire event that occurred in the vicinity of the i5 site.

riod), although southeast and northeast winds also regularly occur (18% and 22% of the studied period, respectively), partly through sea breeze events.

In order to consider the potential influence of meteorology on the bioaccumulation of PAHs and metals in lichens over different integration times, the meteorological TC, RR, RH and WS data were averaged over anteriority periods of 2 days, 15 days, 1, 2, 6 and 12 months before each quarterly sampling. In order to transform the angular nature of wind direction data into continuous numerical variables, the WD were grouped as the relative proportions of the 4 wind sectors NO, NE, SO and SE, all averaged over each of the 6 integration times as well.

As it can be observed on the Fig. 1, TC and RH are clearly negatively correlated, illustrating the seasonal cycle of dry summer periods and milder conditions during the other seasons. Considering the climatic data averaged over the 6 different integration times running from the 10 sampling dates, the negative relation between TC and RH becomes more significant when increasing the integration time from 2 days ( $R = -0.76, p < 0.05$ ) to 6 months ( $R = -0.88, p < 0.001$ ). No correlation was observed on a 12 months integration period ( $R = 0.14$ ), which underlines that RH and TC are correlated on a seasonal basis, but not through their annual running means. All the other significant relations between meteorological parameters imply WD. The NW winds are globally associated to high WS ( $R > 0.68, p < 0.05$  when integrating for 15 days and more). The frequency of SW and NE wind sectors are affected

oppositely by the seasons. The SW wind direction prevails in spring and summer ( $R > 0.71, p < 0.05$  with TC and  $R < -0.76, p < 0.05$  with RH when integrating from 1 to 6 months), with a contribution increasing from 5% in winter to 17% in summer. Meanwhile NE occurs more often in autumn and winter (30%) compared to other seasons (17%), leading to a positive correlation with RH ( $R > 0.74, p < 0.05$  on the 1 to 6 months basis).

### 1.3. Lichen sampling and chemical analysis

The samples were collected at a quarterly frequency during two years to cover seasonality ( $N = 10$ , named T1 to T10, Fig. 1). In addition, the reliability and spatial coverage of the lichen bioaccumulation measurements were estimated during the January 2016 sampling (T6). Therefore, each site benefited from 3 additional sampling spots within less than 500 m distance from the usual spot. The resulting reproducibility would take into account the variability derived from the whole procedure, i.e. sampling, preparation and chemical analysis. It is discussed in the Results section.

The lichen samples consisted of *Xanthoria parietina* full thalli (> 3 cm diameter), collected on at least 5 trees at a height of 1.2 to 2 m. The lichen thalli were rinsed with ultrapure water prior to collection, pulled off the tree bark using ceramic knives and placed away from light at 4 °C until preparation, realized within 24 hr. After the removal of unwanted materials (remaining bark, other lichen species, dust...), they were

**Table 1 – Mean concentrations and standard deviations calculated for the two-year sampling campaign (2015–16, N = 10) in each site.**

Metals (mg/kg dw)	i5	ui1	u3
Al	2875 ± 1068	2015 ± 747	1661 ± 732
V	10.71 ± 3.57	5.91 ± 1.74	3.66 ± 1.40
Cr	35.88 ± 12.72	18.10 ± 8.27	4.66 ± 1.67
Mn	235.5 ± 69.4	72.9 ± 13.9	33.8 ± 9.0
Fe	18184 ± 10224	2912 ± 777	1697 ± 601
Co	1.09 ± 0.37	0.72 ± 0.18	0.55 ± 0.14
Ni	6.39 ± 2.38	3.29 ± 0.81	2.29 ± 0.65
Cu	13.49 ± 8.88	8.61 ± 4.81	8.26 ± 6.25
Zn	65.5 ± 28.5	39.5 ± 13.0	26.0 ± 11.3
As	1.24 ± 1.13	0.87 ± 0.50	0.60 ± 0.36
Mo	3.15 ± 0.94	2.23 ± 0.86	0.96 ± 0.58
Ag	0.18 ± 0.10	0.08 ± 0.11	0.10 ± 0.23
Cd	0.34 ± 0.15	0.20 ± 0.13	0.06 ± 0.08
Sn	3.31 ± 2.19	1.71 ± 1.61	1.62 ± 0.80
Sb	0.85 ± 0.40	0.40 ± 0.23	0.54 ± 0.31
Hg	0.04 ± 0.07	0.28 ± 0.62	0.05 ± 0.14
Tl	0.06 ± 0.06	0.00 ± 0.01	0.00 ± 0.01
Pb	17.19 ± 7.63	6.72 ± 2.99	3.91 ± 1.18
PAHs (µg/kg dw)	i5	ui1	u3
Naphtalene (Nap)	90.3 ± 55.6	31.0 ± 12.0	23.9 ± 6.7
Acenaphtylene (Acy)	44.7 ± 24.7	35.7 ± 27.3	21.0 ± 17.1
Acenaphtene (Ace)	38.2 ± 37.1	54.7 ± 85.5	23.5 ± 18.7
Fluorene (Flu)	39.0 ± 43.3	25.7 ± 43.9	8.1 ± 4.5
Phenanthrene	232.6 ± 118.8	105.7 ± 50.0	61.7 ± 23.6
Anthracene (Ant)	114.7 ± 66.5	220.7 ± 95.0	55.3 ± 13.7
Fluoranthene (FlA)	151.9 ± 71.8	148.1 ± 68.3	63.1 ± 16.8
Pyrene (Pyr)	167.6 ± 162.0	161.7 ± 164.4	84.9 ± 83.2
Benzo(a)anthracene (BaA)	46.8 ± 22.3	38.8 ± 18.9	10.6 ± 6.0
Chrysene (Chr)	104.4 ± 38.3	71.8 ± 33.3	27.3 ± 9.2
Benzo(b)fluoranthene (BbF)	69.3 ± 30.2	67.6 ± 34.0	19.8 ± 7.0
Benzo(k)fluoranthene (BkF)	32.3 ± 17.1	31.8 ± 16.8	15.0 ± 6.3
Benzo(a)pyrene (BaP)	52.7 ± 26.5	61.6 ± 32.2	27.4 ± 14.7
Dibenzo(ah)anthracene (DBA)	41.0 ± 19.0	32.6 ± 23.9	52.6 ± 57.0
Benzo(ghi)perylene (BPe)	50.0 ± 21.7	42.0 ± 14.6	17.3 ± 6.7
Indeno(123-cd)pyrene (IPy)	72.9 ± 45.0	78.5 ± 63.9	36.5 ± 27.3
ΣPAH <sub>16</sub>	1339 ± 326	1199 ± 268	548 ± 124

freeze-dried and finely grounded in a ball mill equipped with ZrO<sub>2</sub> beads and capsules. The samples (approximately 5 g) were then conserved a –40 °C until analysis.

The chemical analysis of PAHs (16 congeners from the USEPA list, see detailed list in Table 1) in the lichen samples (about 2 g) was carried out by GC/MS (Shimadzu QP 2010) equipped with a Zebtron ZB50 column (30 m × 0.25 µm × 0.25 mm, Phenomenex), after an acetone ultrasonic extraction step as described in Ratier et al. (2018). A volume of 1 µL was injected at 250 °C in the spitless mode. The oven temperature program was set as follows: first kept at 100 °C during 1 min, the temperature is increased at 10 °C/min up to 240 °C and then at a rate of 1.5 °C/min up to 280 °C which is hold for 30 min. The quantification is finally realized with the MS detector in the SIM mode, with detection limits of 1 µg/kg for each congener. On the other hand, 18 metal elements (see list in Table 1) were determined in lichen (about 0.5 g) by ICP-MS after microwave acidic mineralization, strictly following the procedure detailed previously in Ratier et al. (2018) with detection limits of 0.1 mg.kg<sup>-1</sup> for each element except As, Cd, Sn and Sb (0.05 mg/kg). The results of

the quality controls by the analysis of certified materials are given in the Supplementary material (Supplementary Materials Table S1).

#### 1.4. Statistical analyses

All the statistical analyses were performed with the R software (version 3.4 or higher, R Core Team, 2020). Hierarchical clustering (“hclust” R function) was used for metals to point out representative clusters of metal elements and reduce the metal data set for further investigations. The clustering was performed with standardized data, employing Euclidean distances and the “ward.d2” criterion (Murtagh and Legendre, 2014).

The influence of the meteorological parameters on the concentration levels of PAHs and metals in lichens, collected during the quarterly samplings in u3, i5 and ui1, was evaluated by means of principal component analysis (PCA, “prcomp” R function using standardized data) linear and multilinear regressions (“lm” R function). Thus, to each of the 10 quarterly samples corresponds 6 averaging time periods (2 days, 15 days,

1, 2, 6 and 12 months) for the 4 climatic parameters temperature TC, rainfall RR, relative humidity RH and wind speed WS (i.e. 24 independent variables) and of the relative contributions of the 4 WD sectors (i.e. 24 inter-dependent variables, as the sum of the 4 sectors, for each of the 6 averaging time periods, necessarily equals to 1), and single PAH and metal concentrations (i.e. 15 dependent variables including at least 90% of detected values, considering individual metal elements and PAHs as  $\Sigma\text{PAH}_{16}$ ).

At first, the relations between the bioaccumulation capacity of lichen and the climatic factors TC, RR, RH, WS, were investigated through the PCA analysis with standardized data. The WD factor was treated separately due to the inter-dependence of the WD sectors relative proportions, that may cause a strong bias in the PCA analysis. Moreover, WD may have a strong impact on the exposure to local sources, such as industrial plumes, introducing additional interference with climatic and seasonal influences. The incidence of WD on lichen bioaccumulation was studied by performing linear regressions, successively for each site, each WD sector and each integration time.

Finally, stepwise multilinear regression analyses were applied, using the backward elimination technique, to evaluate the prevailing influences among seasonal climatic factors and the impacts of WD, possibly favoring specific emission sources, such as local emission plumes and exposure to regional or extra-regional inputs. The analyses included the TC, RR, RH and WS parameters together with the relative contributions of each WD sector, the latter being tested successively, one sector after another, since multicollinearity is expected among wind direction sectors (which necessarily sums to 1). Therefore, to compare among the different models obtained from the different data sets (different wind direction sectors included), the stepwise backward technique was carried out manually. After each regression run, the parameter with the lowest Student *t*-value was eliminated to decrease the global *p*-value, and a new analysis was carried out until 3 variables remained. Then, cross-product terms were additionally considered. The best models were qualified considering global and individual *p*-values, after verification that the residuals fulfilled the Shapiro-Wilk normality test. This work was realized for 2 averaging integration time of each site-contaminant pairs. The integration time considered were chosen regarding the strongest relations with contaminant levels in lichens according to the former PCA (climatic variables) and linear regression (WD) results, with an emphasis to meaningful temporal aspects. In the *ui1* site (Fig. 2), particulate matter (PM<sub>10</sub>) levels were available from the regional air quality network (AtmoSud, 2020) and were included to an additional multilinear regression analysis with the same 6 averaging periods.

## 2. Results and discussion

### 2.1. Spatial and temporal variations in lichen bioaccumulation

#### 2.1.1. Incidence of sites environment

As it is observed worldwide (Domínguez-Moruco et al., 2015; Kodnik et al., 2015; Occelli et al., 2016; Graney et al., 2017;

Boonpeng et al., 2018; Cecconi et al., 2019), and in particular in the investigated area (Dron et al., 2016; Ratier et al., 2018), the bioaccumulation of many metal elements and of PAHs in lichen is enhanced with increasing anthropic pressure, such as urbanization, industrial activity or agriculture. As in previous works, the industrial site *i5* presented the highest levels for all metal elements except Hg, compared to *ui1* and *u3* (Table 1). The *u3* site, theoretically the less exposed site, generally showed the lowest levels, with concentrations 3-fold lower at least for Cr, Mn, Fe, Mo, Cd, Tl and Pb, reflecting the intensity of the anthropic pressure in *i5*, and, to a lesser extent, in *ui1*. PAHs were also highest in lichens sampled from *i5*, but with high discrepancies among congeners compared to *ui1* (Table 1). However, the *u3* site still had concentration levels typically 2 to 3 times lower for all PAH congeners compared to *i5*. Globally, the levels recorded in this area were on the upper end of what observed worldwide, the industrial site *i5* presenting extreme values for most elements and the site *u3* being in the range of typical urban environments even so it is a small town (Domínguez-Moruco et al., 2015; Kodnik et al., 2015; Occelli et al., 2016; Cecconi et al., 2019).

Interestingly, the relative standard deviations calculated from T1 to T10 for metal elements and PAH congeners were comparable for the 3 sites (Table 1), while our previous works showed a higher spatial variability in the vicinity of industrial installations than urban and rural sites (Ratier et al., 2018). This shows that the higher variability observed in industrial sites compared to urban and even more to rural ones, is strictly geographical and associated to the nature of the sampled sites environment.

#### 2.1.2. Spatial reproducibility of bioaccumulation in native *X. parietina*

In January, 2016 (T6), a total of 4 spots were sampled in each of the 3 sites. In the industrial site *i5*, all the spots were composed of poplar and the site topography is very uniform. The average relative standard deviations (RSD) calculated are 24.7% for the 18 metals, and 21.5% for the 16 PAH congeners. Conversely, the spots in the sites *ui1* and *u3* are located in urbanized environments, and present more differences in terms of supporting trees and immediate environments (roadside, park, see Fig. 2). In these sites, the average RSDs are 28.6% and 33.9% for metal elements, respectively. The higher variability observed in the *u3* spots may also be explained by the lower concentration levels measured (Fig. 3), which could induce a higher analytical error. This hypothesis is supported by that the average RSDs, when restricted to elements which concentrations are above 10\*LD, drops to 29.6% in *u3*, while they remain nearly unchanged in *i5* and *ui1* (24.4% and 29.3%, respectively). Singularly, the average RSDs calculated for PAHs are very similar in the 3 sites (between 21.5% and 22.8%), and seem thus less affected by low concentrations than metals (Fig. 2).

Considering the levels of the analytical errors estimated in our laboratory (Ratier et al., 2018) for metals (5%–10%) and PAH congeners (3%–16%), the incidence of the field sampling step on the measurements appears noticeable for metals, while it is surprisingly minor for PAH. Among other, this may be related to different uptake pathways, or to a higher diversity in sources for metal elements compared to PAHs. However, in both cases, the global variability can be considered be-

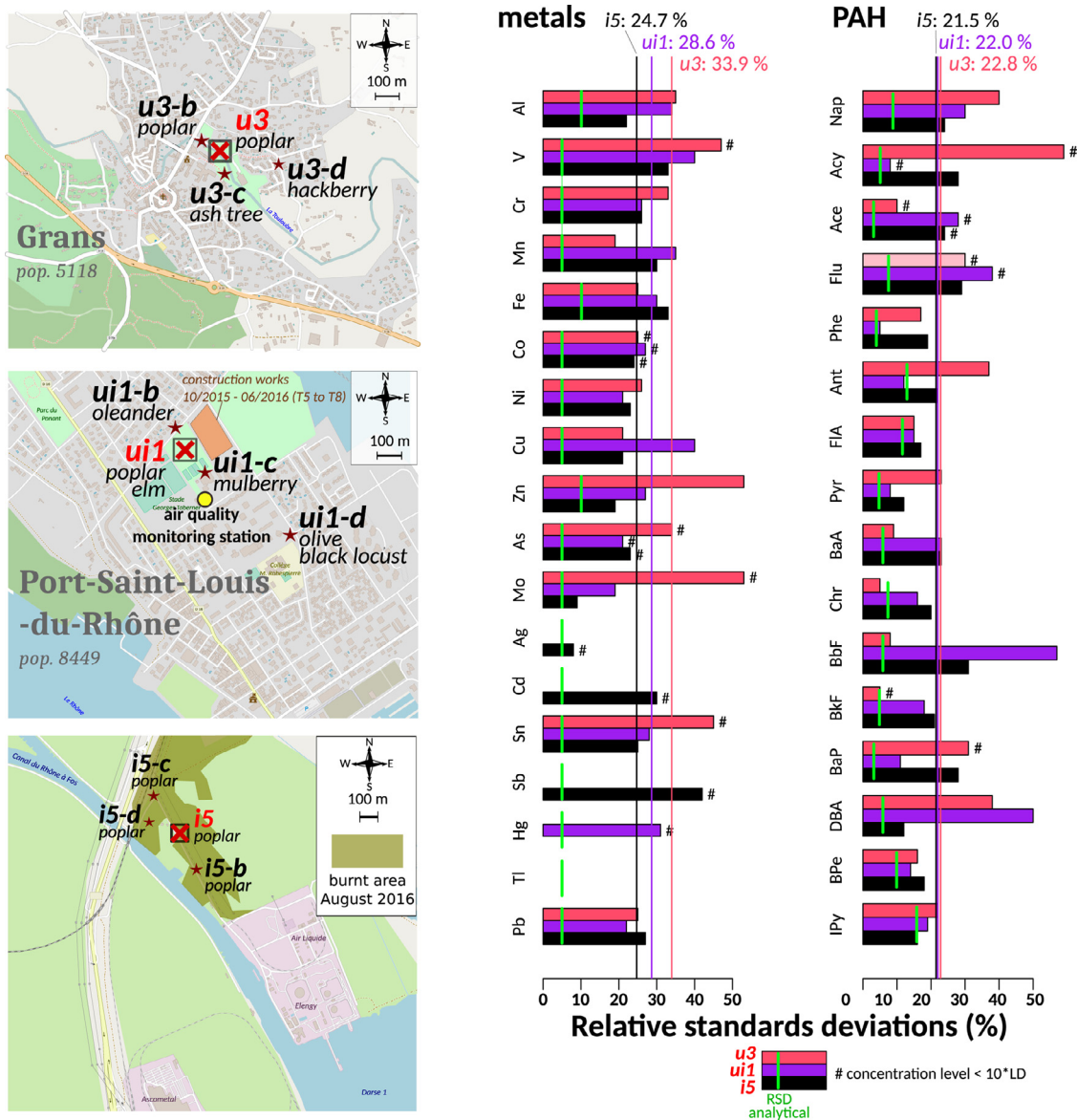


**Fig. 2** – Topographic maps (© OpenStreetMaps) of the sampling sites (red cross in square) and 3 additional spots (burgundy stars) investigated at T6 for spatial reproducibility evaluation (left), and relative standard deviation (RSD) results of the analyses of the contaminants ( $N = 4$ ). Mean RSDs across all metals and PAH congeners are also materialized by the plain lines (pink, purple and black for u3, ui1 and i5, respectively), and low concentration levels ( $< 10^*LD$ ) are marked by an “#”. Calculated analytical errors are indicated by the discontinued green lines (For interpretation of the references to color in this figure legend, the reader is referred to the web version of this article.).

low 30% when comfortable analytical conditions are reached (concentration  $> 10^*LD$ ), which remains very satisfying. It also shows that the lichen bioaccumulation measurements are representative in the perimeter studied here, i.e. 500 m diameter, and not significantly affected by different supporting trees and topology, which is consistent with previous works on other fruticose lichen species for PAHs (Kodnik et al., 2015) and metals (Adams and Gottardo, 2012).

**2.1.3. Temporal variations of PAHs and metals concentrations**  
The evolution of the PAHs and metals concentrations in lichen were studied during a two-year period, beginning in January,

2015 through October, 2016. Winter samples (T1, T2, T6, T7) are slightly over-represented in comparison to autumn (T5, T10), spring (T3, T8) and summer (T4, T9). The evolution of the concentrations is shown in Fig. 3 along with daily mean temperatures, for a seasonal indication purpose.

A hierarchical clustering analysis was employed to group metal elements according to comparable variability from T1 to T10 (see Fig. S2). The elements V, Cr and Zn, representative of petrochemical activities (Sylvestre, 2016), are well clustered together, as well as Ni, Pb, and Co. The elements Mn and Fe, which are characteristic of steel industry in this area (Sylvestre et al., 2017), are sharply associated, and also close

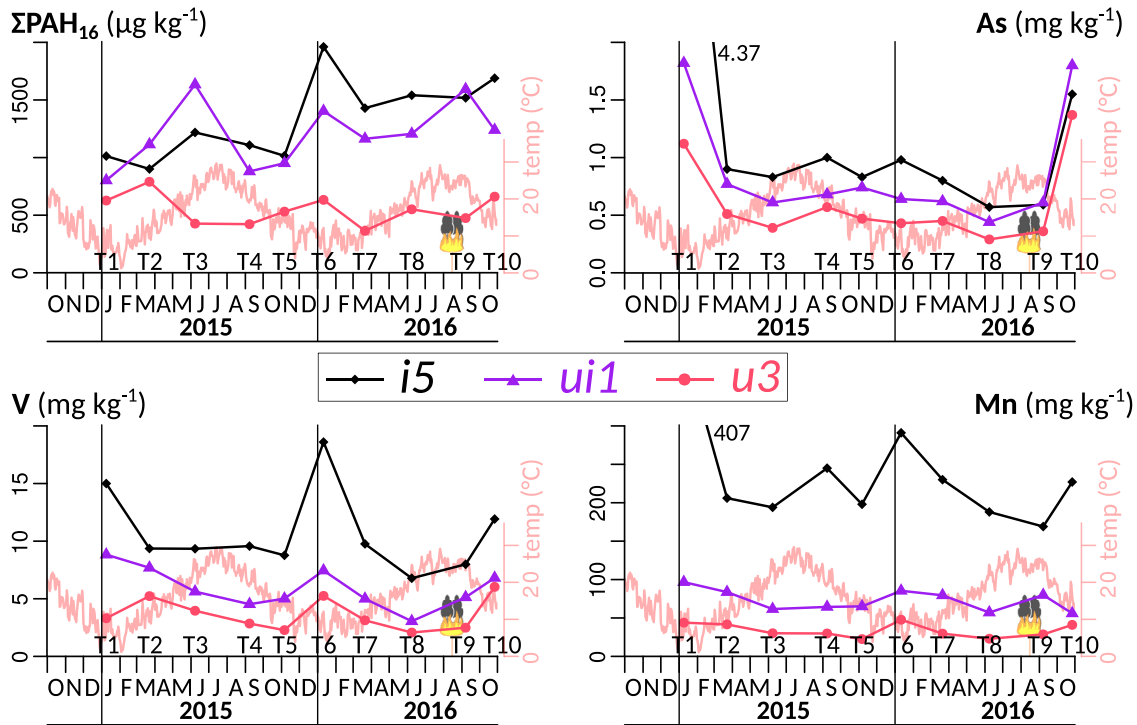


**Fig. 3 – Evolution of concentrations of PAH and metals in *X. parietina* lichen samples during the 2 years of the study. The fire pictogram marks the date of the 711 Ha forest fire around i5.**

to the V and Ni groups possibly due to the proximity of both industries in the neighborhood of sites i5 and ui1. A third group gathers As, Al, Cd, Sn and Sb with a looser aggregation level. Interestingly the clusters are similar to that of a wider campaign including 24 other sites in the same territory (Ratier et al., 2018). This corroborates that the 3 sites monitored in the present study are representative of the area.

Nearly all the contaminants concentrations are globally stable over the whole two-year period, except PAHs in both the i5 and ui1 sites which present an increasing trend from T1 to T10. This apparent annual stability hides greater variations between specific sampling times. For most metal elements such as V, Mn and, in a lesser extend, As (Fig. 3, Table S3), the concentrations are generally higher in winter and autumn than in summer or spring. The contrast between the highest and lowest levels ranges from a factor 2 to 8-fold in all 3 sites, according to the element, which is much higher than the variability induced by sampling and analysis. The pattern is similar for ΣPAH<sub>16</sub> when ignoring the general increase of the concentrations in ui1 and i5, but with lower differences (factors of 2.2, 1.9 and 2.2 for the i5, ui1 and u3 sites, respectively).

These observations support that sampling should be realized within the shortest period of time, and in any case limited to less than a few weeks. As observed in a few previous studies (Augusto et al., 2013; Kodnik et al., 2015), a seasonal effect had a clear incidence on the contaminants concentrations measured in native *X. parietina* lichen samples, with globally higher levels in winter and autumn. This is consistent with recent observations carried out with transplanted lichens (Rola et al., 2020; Capozzi et al., 2020). Conse-

quently, comparisons of multi-annual data should definitely take into account the seasonal aspects, working with indigenous lichens as with transplants.

**2.1.4. Impact of specific events (forest fire, construction works)**

Two unintended events occurred during the two-year period of the study, which could affect the lichen bioaccumulation of at least several atmospheric contaminants. We report here all the observations, and discuss the impacts in terms of PAH and metal concentrations.

The main event was a major forest fire (711 Ha total burnt surface, on 10/08/2016), which took place in the industrial area around the site i5, 3 weeks before the sampling date T9 (Figs. 1 and 3). It also devastated approximately 80% of the trees of the sampling site i5 (Fig. 2). The fire occurred under northwesterly strong winds (40 to 80 km/hr) and started about 1 km north from i5, extending further south and east, and lasting for a total of about 24 hr. From these information, it can be considered that the fire did not remain active for more than a few hours in i5, near from where it started. It can be observed that no change occurred in terms of ΣPAH<sub>16</sub> in sites u3 and i5, but slightly increased in ui1. More precisely, a significant increase of the PAH congeners concentrations with 4 (BaA, Chr) and 5 (BbF, BkF, BaP) aromatic rings was noted, presenting their highest values at T9 among the two-years study period in ui1 and i5, while their levels remained as usual in u3 (Table S3). The site ui1, located only 3 km south away from the burnt area, and i5, devastated by fire, were exposed to the fire plumes, while the site u3 is 20 km northeast and was very unlikely exposed. The concerned PAH congener levels in ui1 and i5 came back to regular values at the subsequent sampling date T10. The

very brief forest fire event appeared to have a noticeable impact at the PAH congener level, while rather minor considering  $\Sigma\text{PAH}_{16}$ , since the 5 congeners incriminated were not prominent in the  $\Sigma\text{PAH}_{16}$ , contributing to 21% and 22%, in *ui1* and *i5*, respectively. On the other hand, the concentrations of metals in *X. parietina* did not show any significant variation at T9 compared to other samplings (Table S3), which is consistent with that metals are not substantial in biomass burning emissions (Pernigotti et al., 2016).

Also, the sampling site *ui1* was affected by a nearby (< 200 m) construction work for an approximately 500 student capacity high school, during 8 month with various operating stages (October 2015 to July 2016, covering T5 to T8). Even though a strong increase in PAHs was observed at T6 in *ui1*, it was also observed in *u3* and *i5*, while the emissions expected from such construction works are not expected to affect distances exceeding a few km. A similar trend was observed for most metals, and all concentrations decreased at T7. The temporary increase in PAHs at T6 could be thus more reasonably attributed to a regional scale increase, possibly due to climatic or physiologic aspects. And the construction works near the site *ui1*, probably did not have any significant consequences on contaminants bioaccumulation.

## 2.2. Influence of meteorological and environmental conditions

### 2.2.1. Relations between climatic conditions and lichen bioaccumulation

The impact of the climatic parameters on contaminants bioaccumulation in lichen may be affected by a certain inertia. Therefore, the principal component analysis (PCA) was realized with the whole set of contaminants in the 3 sites and climatic parameters (TC, RR, RH and WS) at various integration time before each sampling (2 days, 15 days, 1 month, 2 m, 6 m and 12 m). Note that wind direction (WD) was not included in the analysis at this stage, as justified in Section 2.3. The detailed loadings of the PCA factors, including climatic parameters and contaminant levels, are presented in Table 2 for the three main components, accounting for a cumulative 72.7% of the total variability.

The PCA analysis advantageously depicts main components that reflect distinct seasonal and climatic characteristics. The main component, explaining nearly half of the variability (44.2%), clearly distinguishes the influence of high humidity (RH) conditions associated to mild temperatures (TC), in particular at short (2 and 15 days) and mid-term (1 and 2 months) time integrations. These conditions are representative of the winter and spring seasons, as well as late autumn. Also, we considered this component as of seasonal influence, in which higher concentrations of all the metal elements are associated to elevated RH (Table 2). These higher levels observed in winter were not associated to global or regional atmospheric effects in winter (e.g. narrower atmospheric boundary layer), as local PM<sub>10</sub> levels were not especially higher in winter during this period (see Fig. S4, AtmoSud, 2020). Also, biomass burning emissions, which are mainly limited to winter, do not significantly contribute to metal emissions (Pernigotti et al., 2016; Sylvestre, 2016). Thus, the higher bioaccumulation levels affecting all metal elements in winter and mild seasons sug-

gest an influence from physiological aspects. Humid and mild climatic conditions have been shown to favor the growth of *X. parietina* in a comparable Mediterranean region (Fortuna and Tretiach, 2018), and thus may be expected to enhance their bioaccumulation capabilities. The PAH levels in sites *i5* and *ui1* seem little dependent of this component, potentially due to strong local sources from industrial and shipping activities which could prevail over seasonal factors.

The second component, which drops to a contribution of 17.4% of the total variability, mainly points out the wind speed (WS) conditions. As expected, for most contaminants, as well as for RH (short and mid-term), the levels are not related or negatively correlated with WS. In particular, PAHs in the sites *i5* and *ui1* are strongly associated to low WS, which appears prominent in both sites compared to seasonal TC and RH variations. As high WS is associated to northwesterly winds, this results may be the consequence of that main emission sources are located downwind from other directions, mostly to the east in these sites. On the other hand, noticeable exceptions are the metal elements As, Sn, Sb and Pb in sites *i5* and *ui1* (Table 2). For these few elements, an influence from local and specific sources in the north can be considered among other possibilities.

Finally, the action of rainfall (RR) intensity on bioaccumulation of metals and PAHs is illustrated by the third component, which accounts for 11.0% of the total variability. As RR is associated to high RH and low TC, this component is mixed with the seasonal aspect. While other studies did not observe significant correlations (either positive or negative) between contaminant bioaccumulation in lichen and RR (Bergamaschi et al., 2007; Malaspina et al., 2014), this “rain/seasonal” component has either a negative or no influence on PAH and metal elements levels, despite it is associated to high RH. Molybdenum (Mo) in the *ui1* and *i5* sites makes an exception (Table 2). The only significant atmospheric source of Mo is, to our knowledge (Dron and Chamaret, 2015), a chemical plant which is located between *i5* (3 km to the south) and *ui1* (5 km to the northeast). It was clearly identified in lichens sampled in its vicinity during a previous study (Ratier et al., 2018), and its specificity, being a fixed, unique and very local source, may interfere with climatic aspects in the present interpretations.

The integration time did not show a strong impact on these 3 first components, as the factors of the different climatic parameters were relatively homogeneous through the length of time integration. Still, RH, which is positively correlated to most contaminants variability in the first component, shows a greater effect when integrating for a 1 or 2 months period of time, consistently with seasonal variations, identified as this component feature (Table 2).

### 2.2.2. Impact of wind direction

In order to analyze statistically the influence of WD, its angular nature was transformed to continuous numerical values corresponding to wind sectors relative contributions. As a consequence, the WD data became inter-dependent (total equals to 1) and could not be included into the PCA analysis. Therefore, linear regressions were applied to identify potential correlations with PAHs and metal elements concentrations in lichen, for each site-integration time pair. The results for PAHs



**Table 2 – Eigen values (loadings) for the 3 main components of the principal component analysis (PCA) including the meteorological parameters (at 12, 6, 2, and 1 month and 15, and 2 days integration times) and the contaminant concentrations (in sites u3, ui1 and i5). The meteorological features were determined according to the Eigen values obtained for the meteorological parameters.**

Components (variance explained)	PC1 (44.2%)	PC2 (17.4%)	PC3 (11.0%)
<b>Meteorological feature</b>	<b>Seasonal</b>	<b>Wind</b>	<b>Rain/Seasonal</b>
<b>Meteorological parameters</b>	<b>PC1 loadings</b>	<b>PC2 loadings</b>	<b>PC3 loadings</b>
Rainfall long-term (12 m/6 m/2 m)	-0.07/-0.12/-0.07	0.07/0.07/0.16	-0.14/-0.21/-0.20
Rainfall short-term (1 m/15 d/2 d)	0.03/ns/0.02	0.02/ns/ns	-0.21/-0.27/-0.20
Temperature long-term (12 m/ 6m/2 m)	-0.06/ns/0.12	0.11/0.01/0.06	0.13/0.17/0.21
Temperature short-term (1 m/15 d/2 d)	<b>0.13/0.15/0.14</b>	0.04/0.03/0.02	<b>0.18/0.13/0.14</b>
Wind speed long-term (12 m/6 m/2 m)	-0.01/0.04/ns	<b>0.12/0.18/0.19</b>	-0.10/0.02/-0.11
Wind speed short-term ( 1m/15 d/2 d)	-0.01/-0.08/0.04	<b>0.25/0.20/0.08</b>	-0.08/0.12/0.24
Rel. humidity long-term (12 m/6 m/2 m)	-0.09/-0.08/-0.14	0.14/-0.01/-0.08	-0.06/-0.18/-0.13
Rel. humidity short-term (1 m/15 d/2 d)	-0.12/-0.08/-0.08	-0.15/-0.16/-0.11	-0.09/-0.17/-0.20
<b>Contaminants</b>	<b>PC1 loadings</b>	<b>PC2 loadings</b>	<b>PC3 loadings</b>
PAH (u3/ui1/i5)	-0.10/0.05/0.02	-0.03/-0.14/-0.23	-0.11/0.09/0.14
Al (u3/ui1/i5)	-0.15/-0.14/-0.16	-0.09/0.08/0.07	-0.06/-0.11/0.08
V (u3/ui1/i5)	-0.09/-0.17/-0.15	<b>0.10/ns/-0.14</b>	-0.04/-0.01/0.10
Cr (u3/ui1/i5)	-0.15/-0.12/-0.15	-0.11/-0.19/-0.11	ns/0.01/0.12
Mn (u3/ui1/i5)	-0.16/-0.14/-0.16	-0.08/-0.01/0.04	0.04/ns/0.10
Fe (u3/ui1/i5)	-0.16/-0.14/-0.14	-0.06/0.04/0.07	0.04/-0.03/0.13
Co (u3/ui1/i5)	-0.17/-0.12/-0.16	0.01/0.11/0.10	0.03/-0.05/0.09
Ni (u3/ui1/i5)	-0.17/-0.14/-0.15	0.01/-0.01/0.11	0.01/-0.07/0.08
Cu (u3/ui1/i5)	-0.10/-0.11/-0.12	-0.23/-0.21/-0.19	0.08/0.01/0.11
Zn (u3/ui1/i5)	-0.17/-0.13/-0.16	-0.05/0.01/-0.03	<b>0.10/-0.06/0.17</b>
As (u3/ui1/i5)	-0.09/-0.11/-0.14	<b>0.10/0.11/0.14</b>	0.09/0.09/0.10
Mo (u3/ui1/i5)	-0.11/-0.06/-0.12	-0.21/0.01/0.05	-0.02/-0.22/-0.14
Sn (u3/ui1/i5)	-0.16/-0.14/-0.14	-0.05/0.15/0.15	<b>0.12/0.07/0.11</b>
Sb (u3/ui1/i5)	-0.14/-0.08/-0.13	-0.17/0.25/0.17	0.09/-0.04/0.08
Pb (u3/ui1/i5)	-0.17/-0.14/-0.14	0.02/0.13/0.15	0.03/0.04/0.06

Bold values indicate the Eigen values above average (absolute values of 0.11, 0.10 and 0.10 for PC1, PC2 and PC3, respectively). ns = not significant; m = month; d = day.

and the most relevant metals, representative of the main clusters identified previously (Fig. S2), are presented in Fig. 4.

In the sites ui1 and u3, integration times of 1 and 2 months present the best relations, including the most significant ( $p < 0.01$ ) and nearly all the positive correlations. In both sites, they strictly concern metal elements, which positively correlate with the northeast sector wind frequencies. This is consistent with the localization of the major industrial installations toward site ui1, and of the urban area of Salon-de-Provence (population approx. 45,000) toward site u3 (Fig. 1). Note that all the contaminant levels are much lower in u3. However, the collinearity of the NE winds with RH might also have driven this correlation (or vice versa), in particular on the 1 and 2 month integration basis.

Significant correlations are observed in the site i5, for most integration times, from 15 days to 12 month. The positive correlations appear with the southeast and northeast sectors. This is consistent with the fact that the i5 site is located within the industrial zone, with most industries located to the southeast and urban areas to the east. Curiously, metal elements are associated to northeast winds on a 1–2 month integration basis and southeast for 12 month integration time, while PAHs present an opposite pattern. As for sites ui1 and u3, the correlations with NE could be related to the seasonality of this wind sector. On the other hand, the correlations between contaminants and the SE wind sector seem better associated to the industrial emissions.

Integrating wind sectors frequencies, one by one, to the other meteorological parameters in multiple linear regression analyses should give an indication of the contributions of WD to the contaminant bioaccumulation in lichen, compared to the other climatic parameters.

2.2.3. Comparison of the wind direction and other climatic parameters

Table 3 presents the predicting variables entering the best models obtained for each site-integration time pair, on the basis of optimized  $p$ -values. Including the climatic parameters (TC, RH, RR and WS) to the WD sectors (WDXX) in multilinear models slightly increases the number of significant results. Among all the site-integration time pairs, 74% obtain a global model  $p < 0.05$ . Only 4 site-integration time pairs present their best correlations with a single parameter, that are negative correlations between Ni and WDSW in u3 and ui1 on 2 and 12-month integration time, respectively, and between PAHs and RR in ui1 and i5 for 1 and 12 month integration time, respectively. The inclusion of several environmental parameters in most of the best models highlights the relevance of taking into account their complex and interacting nature towards the bioaccumulation of pollutants in native lichens.

Globally, WD is the most represented parameter, regardless of a specific direction, and appears in 52% of the site-time pairs. Among the 4 sectors, negative correlations with SW winds prevail, in particular in the sites u3 and ui1. This is

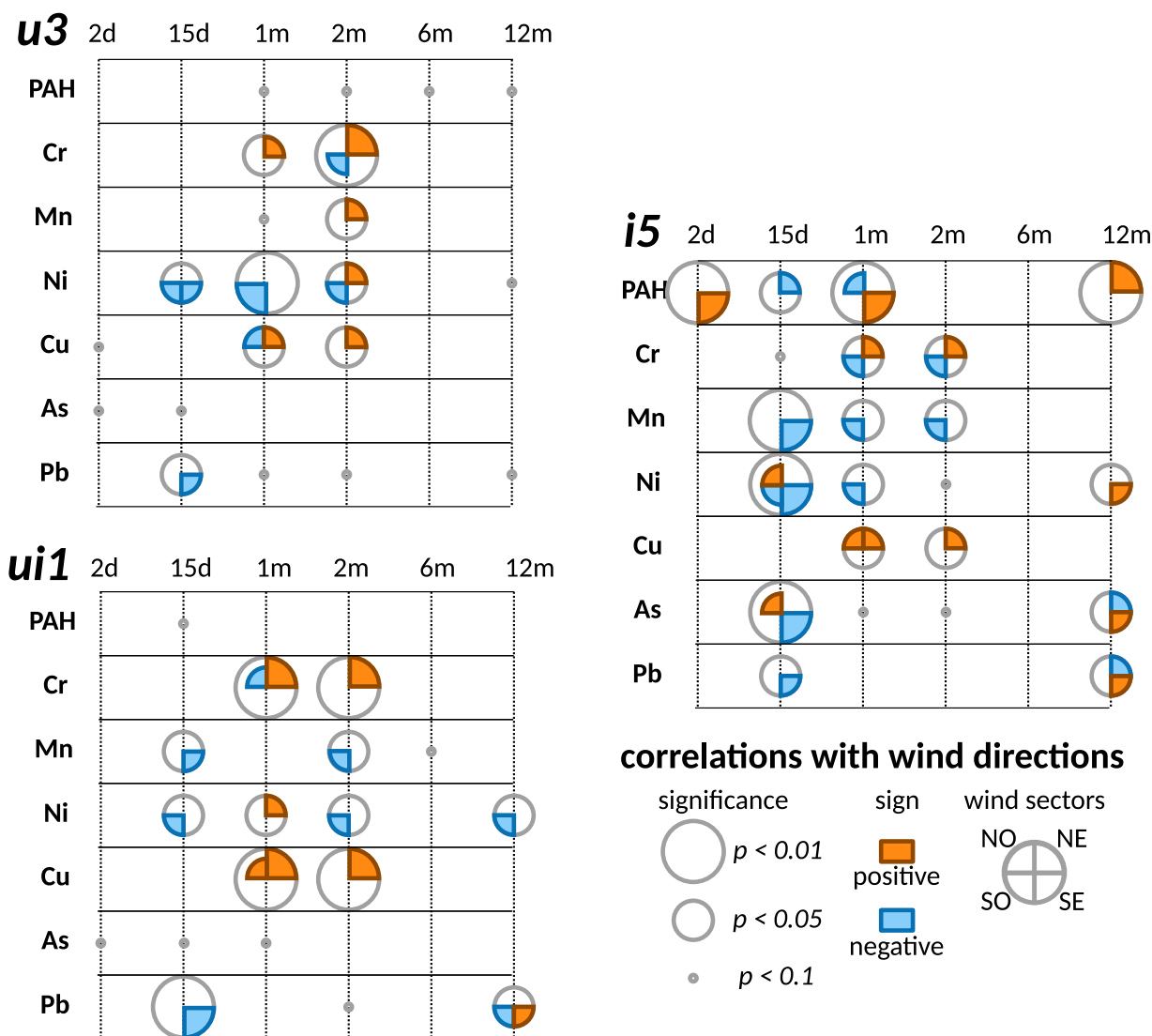


**Fig. 4 – Significance results of single linear correlations between the proportions of the different wind sectors and contaminants levels. m = month; d = day.**

consistent with the main local atmospheric emission sources, among which none are located to the southwest of the sites, as indicated previously. All the stepwise regressions reached significant models in site i5, but only to 6 out of 14 in u3. This underlines that u3 is less impacted by WD and local sources, but rather to regional air pollution events inducing lower accumulation levels.

Approximately 40% of the best regressions include the rain intensity parameter RR, predominantly as a negative impact on concentration levels, which is consistent with the previous PCA results. Its influence is particularly prevailing towards PAH concentrations in sites ui1 and i5, next to the industrial activities. The WS factor is also present in a large number of site-integration time pairs models, but its incidence is generally secondary in comparison to other parameters constituting the model. Accordingly, it often appears where WD is prevalent, as a probable consequence of the association of WS with WD.

Finally, the inclusion of WD sectors in the statistical analysis relegates the RH and TC factors to minor contributions,

appearing in less than 20% of the retained models among the 42 site-integration time pairs. This likely shows that the seasonal factor does have a strong impact on the bioaccumulation levels in *X. parietina* lichens, but clearly becomes minor when sites are regularly exposed to elevated atmospheric contaminant concentrations, which are often favored under specific WD conditions. It is noteworthy that the prevailing influence of WD becomes more significant when approaching the vicinity of strong atmospheric emission sources, such as in ui1 and i5.

#### 2.2.4. Incidence of PM10 levels

The lichen sampling site ui1 is located by an atmospheric monitoring station (150 m distance, Fig. 2) including particulate matter on-line measurements (PM10), operated by the local air quality monitoring network (Atmosud, 2020). In the same way as for WD, the PM10 data were added to the ui1 dataset for multilinear regressions to explore its incidence on the bioaccumulation of PAHs and metals in *X. parietina*. The integration time basis was the same as for the other meteorological

**Table 3 – Results of stepwise backward multilinear regressions. Best models obtained are presented, through their global *p*-value (rank, bold signs) and the individual variables *p*-values included in the achieved models. Variables are listed from top to bottom according to decreasing Student *t*-values. (+) and (-) signs indicate positive and negative correlations, respectively.**

site	u3		ui1		i5	
Integration time	2 m	12 m	1 m	12 m	1 m / 2 m	12 m
PAH	* (+)WDNE * (+)WS *	* (-)WDSW * (-)RR *	* (-)RR *	* (-)TC * (+)WDSW * (+)RH .	<b>***2 m</b> (-)RR *** (+)RH **	** (-)RR**
Cr	** (-)WS *** (+)WS:RR *** (-)RR ***	ns	** (+)WDNE *** (-)RR.	. (+)RR * (-)RR:WS * (+)WS .	<b>**2 m</b> (+)RH ** (+)TC ** (-)TC:RH *	** (+)RR ** (-)RR:WS ** (+)WS **
Mn	* (+)RR:WS ** (-)RR** (-)WS **	ns	* (-)TC * (+)WDSW:TC * (-)WDSW *	* (-)WDSW * (-)WS *	<b>**2 m</b> (+)RH ** (-)RH:RR ** (+)RR ** (-)WDSE **	** (+)RR ** (-)RR:WS ** (-)WDNE * (+)WS *
Ni	* (-)WDSW *	ns	* (+)TC * (+)RH * (-)TC:RH *	* (-)WDSW *	<b>**1 m</b> (-)WDSW ** (-)RR * (+)WS * (+)WDSO:RR *	** (-)WDSW ** (+)TC ** (-)WS .
Cu	** (+)WDNE *** (-)WDNE:RR * (+)RR .	ns	** (+)RH:WDNE * (-)RH * (-)WDNE *	ns	<b>***1 m</b> (+)WDSE *** (-)WDSE:WS *** (+)WS **	** (+)RR ** (-)RR:WS ** (+)WS ** (+)WDNE.
As	ns	ns	ns	ns	<b>**2 m</b> (+)WDSE:RH ** (-)WDSE ** (-)RH **	** (-)RH ** (+)RH:WDSE ** (-)WDSE **
Pb	ns	ns	* (-)WDSW * (+)WS * (-)RR *	** (-)WDSW ** (-)WS * (+)TC .	<b>**1 m</b> (-)WDSW ** (+)WS ** (-)RR ** (+)WDSW:RR *	** (-)WDNE *** (-)WS *** (+)RR **

Signif. codes: 0 < \*\*\* < 0.001 < \*\* < 0.01 < \* < 0.05 < . < 0.1 < 'ns' 1. m = month.

logical parameters (2 day, 15 day, 1 month, 2 month, 6 month and 12 month), for an homogeneity purpose. It was restricted to ui1, as no PM monitoring station is located at a suitable distance from i5 or u3 and that monitoring stations may not be representative of PM10 levels occurring several kilometers away.

The inclusion of the PM10 parameter in the site ui1 particularly improved the quality of the model for PAHs, on a 1 month integration time basis. A very low *p*-value was obtained for the global model (0.0007, \*\*\*), as well as for its composing parameter PM10 (*p* < 0.001), and to a lesser extent TC (*p* < 0.01) and RR (*p* < 0.05). On the other hand, no improvement could be achieved for the 12 month integration time.

In the case of most metals (Cr, Mn, Ni, Cu), the addition of PM10 in the regression analysis did not enhance the results. Only slightly better correlations were observed in ui1 for As (12 month integration time, (-)PM10\* (+)WDSW, global *p* < 0.05) and Pb at both 2 ((+)WDNW\*\* (-)WDNW:PM10\*\* (+)PM10\*\* (+)RH\*, global *p* < 0.01) and 12 month ((+)WDSE\*\* (-)WDSE:PM10\*\* (+)PM10\*\*, global *p* < 0.001) integration time.

Globally, it can be concluded that the addition of the PM10 parameter does not drastically improve the description of

bioaccumulated contaminant levels through multilinear regression, except for PAHs on a 1 month integration time basis. Several hypothesis could be formulated, such as the role of the bioaccessibility of the contaminants into bioaccumulation (chemical speciation, particle size) or physiological aspects of lichens (growth rate, elimination) prevailing over global pollution. Also, PM10 may not necessarily describe consistently metal and PAH atmospheric levels in the studied area. The peculiar aspect of PAHs contamination in the site ui1 has been evoked before (see Section 3.1.3.), and the strong association of PAH levels in lichens sampled in ui1 with collocated PM10 levels (for 1 month integration time) could be an interesting basis for future research.

### 3. Conclusions

In order to improve the knowledge toward the parameters that influence the bioaccumulation levels in native lichens, and with the ambition of supporting the adjustment of future monitoring protocols, a two-year sampling campaign was carried out in three contrasted sites, including quarterly sam-

plings and an evaluation of the sampling uncertainty. Additionally, a specific attention was given to the impacts of unintended events such as forest fire or nearby construction works.

Assuming comfortable analytical conditions (concentration levels > 10\*LD), it was calculated that the measurement of PAHs and metals bioaccumulation in *X. parietina* native lichen was meaningful within at least a 500 m perimeter and a variability below 30%. In that respect, the relative reproducibility was found to be mainly affected by low concentration levels leading to stronger uncertainties, but only marginally by topography and supporting trees.

Unexpected events may happen during lichen sampling campaigns. We experienced two different types of situations by the study sites during the two-year monitoring, an intense but very brief event (forest fire), and a nearby activity with a relatively limited spatial scale (construction works). Globally, these episodes did not induce significant variations in PAHs and metals bioaccumulation levels, but a slight and temporary increase in a few PAH congeners was observed after the forest fire in the concerned sites.

Seasonal effects were highlighted, in relation to climatic parameters. The bioaccumulation of contaminants was favored by a high relative humidity and mild temperatures, while strong winds and rainfall had a slight negative incidence. Under Mediterranean climate, this implies that higher concentration levels may be measured from late autumn to early spring.

The wind direction has theoretically no incidence on the lichen capacities to bioaccumulate pollutants, when pollution sources are equally distributed around the sampling sites. In field conditions, it is rarely the case, and the relative influence of local emissions compared to climatic parameters such as humidity, temperature and rainfall, may be affected by the wind direction parameter. This study showed that the incidence of wind direction prevailed over climatic parameters in the vicinity of large local emission sources such as heavy industrial installations, but could become minor in more remote areas. This difference among sites environment may have an incidence on the results of lichen biomonitoring, upon the season chosen for sampling.

The study also showed that seasonal effects are integrated by lichens within a few months, while a changing contamination level may be reflected within a larger integration time up to 12 months at least.

Thus, it is highly recommended to carry out lichen sampling in the same season when aiming to inter-annual comparison purposes, for instance, and at least to systematically consider seasonal effects when discussing lichen bioaccumulation data. On the other hand, native lichen biomonitoring reliability was also confirmed when used to evaluate air quality on a large time-scale, with a high level of reproducibility and only little influence from temporary events.

## Acknowledgments

The authors gratefully acknowledge Meteo-France for providing the meteorological data, through the research agreement DIRSE/REC/16/02/0.

This work was fully funded by the “Institut Écotoxicologique pour la Connaissance des Pollutions”.

## Supplementary materials

Supplementary material associated with this article can be found, in the online version, at [doi:10.1016/j.jes.2021.03.045](https://doi.org/10.1016/j.jes.2021.03.045).

## REFERENCES

- Adams, M.D., Gottardo, C., 2012. Measuring lichen specimen characteristics to reduce relative local uncertainties for trace element biomonitoring. *Atmos. Pollut. Res.* 3 (3), 325–330.
- Alves, C.A., Vicente, A.M., Custódio, D., Cerqueira, M., Nunes, T., Pio, C., et al., 2017. Polycyclic aromatic hydrocarbons and their derivatives (nitro-PAHs, oxygenated PAHs, and azaarenes) in PM<sub>2.5</sub> from Southern European cities. *Sci. Total Environ.* 595, 494–504.
- Atmosud, 2020. Monitoring stations and data. <https://www.atmosud.org/donnees/acces-par-station>
- Augusto, S., Pereira, M.J., Máguas, C., Branquinho, C., 2013. A step towards the use of biomonitors as estimators of atmospheric PAHs for regulatory purposes. *Chemosphere* 92 (5), 626–632.
- Augusto, S., Sierra, J., Nadal, M., Schuhmacher, M., 2015. Tracking polycyclic aromatic hydrocarbons in lichens: it's all about the algae. *Environ. Pollut.* 207, 441–445.
- Bargagli, R., Iosco, F.P., Barghigiani, C., 1987. Assessment of mercury dispersal in an abandoned mining area by soil and lichen analysis. *Water Air Soil Pollut.* 36 (1–2), 219–225.
- Bergamaschi, L., Rizzio, E., Giaveri, G., Loppi, S., Gallorini, M., 2007. Comparison between the accumulation capacity of four lichen species transplanted to a urban site. *Environ. Pollut.* 148 (2), 468–476.
- Boamponsem, L.K., de Freitas, C.R., Williams, D., 2017. Source apportionment of air pollutants in the Greater Auckland Region of New Zealand using receptor models and elemental levels in the lichen, *Parmotrema reticulatum*. *Atmos. Pollut. Res.* 8 (1), 101–113.
- Boonpeng, C., Sriviboon, C., Polyiam, W., Sangiamdee, D., Watthana, S., Boonpragob, K., 2018. Assessing atmospheric pollution in a petrochemical industrial district using a lichen-air quality index (LiAQI). *Ecol. Indic.* 95, 589–594.
- Capozzi, F., Sorrentino, M.C., Di Palma, A., Mele, F., Arena, C., Adamo, P., et al., 2020. Implication of vitality, seasonality and specific leaf area on PAH uptake in moss and lichen transplanted in bags. *Ecol. Indic.* 108, 105727.
- Carlberg E., Georg, Ofstad B., Elizabeth, Drangsholt, Hilde, Steinnes, Eiliv, et al., 1983. Atmospheric deposition of organic micropollutants in Norway studied by means of moss and lichen analysis. *Chemosphere* 12 (3), 341–356.
- Ceccconi, E., Fortuna, L., Benesperi, R., Bianchi, E., Brunialti, G., Contardo, T., et al., 2019. New interpretative scales for lichen bioaccumulation data: the Italian proposal. *Atmosphere* 10 (3), 136 (Basel).
- Contardo, T., Vannini, A., Sharma, K., Giordani, P., Loppi, S., 2020. Disentangling sources of trace element air pollution in complex urban areas by lichen biomonitoring. A case study in Milan (Italy). *Chemosphere* 256, 127155.
- Dauphin, C.E., Durand, A., Lubonis, K., Wortham, H., Dron, J., 2020. Quantification of monosaccharide anhydrides by gas chromatography/mass spectrometry in lichen samples. *J. Chromatogr. A* 1612, 460675.
- Domínguez-Morueco, N., Augusto, S., Trabalón, L., Pocurull, E., Borrull, F., Schuhmacher, M., et al., 2015. Monitoring PAHs in the petrochemical area of Tarragona County, Spain:

- comparing passive air samplers with lichen transplants. *Environ. Sci. Pollut. Res.* 24 (13), 11890–11900.
- Dörter, M., Karadeniz, H., Saklangıç, U., Yenisoay-Karakaş, S., 2020. The use of passive lichen biomonitoring in combination with positive matrix factor analysis and stable isotopic ratios to assess the metal pollution sources in throughfall deposition of Bolu plain, Turkey. *Ecol. Indic.* 113, 106212.
- Dron, J., Chamaret, P., 2015. Investigating Molybdenum Emissions from the Lyondell Chimie France industrial Site in Fos-sur-Mer. Final report. Institut Ecocitoyen Pour La Connaissance des Pollutions, Fos-sur-Mer (France) [www.institut-ecocitoyen.fr](http://www.institut-ecocitoyen.fr).
- Dron, J., Austruy, A., Agnan, Y., Ratier, A., Chamaret, P., 2016. Biomonitoring with lichens in the industrialo-portuary zone of Fos-sur-Mer (France): feedback on three years of monitoring at a local collectivity scale. *Pollut. Atmos.* 228, 2268–3798.
- Fortuna, L., Tretiach, M., 2018. Effects of site-specific climatic conditions on the radial growth of the lichen biomonitor *Xanthoria parietina*. *Environ. Sci. Pollut. Res.* 25 (34), 34017–34026.
- Godinho, R.M., Wolterbeek, H.T., Verburg, T., Freitas, M.C., 2008. Bioaccumulation behaviour of transplants of the lichen *Flavoparmelia caperata* in relation to total deposition at a polluted location in Portugal. *Environ. Pollut.* 151 (2), 318–325.
- Godinho, R.M., Verburg, T.G., Freitas, M.C., Wolterbeek, H.T., 2009. Accumulation of trace elements in the peripheral and central parts of two species of epiphytic lichens transplanted to a polluted site in Portugal. *Environ. Pollut.* 157 (1), 102–109.
- Graney, J.R., Landis, M.S., Puckett, K.J., Studabaker, W.B., Edgerton, E.S., Legge, A.H., Percy, K.E., 2017. Differential accumulation of PAHs, elements, and Pb isotopes by five lichen species from the Athabasca Oil Sands Region in Alberta, Canada. *Chemosphere* 184, 700–710.
- Kodnik, D., Carniel, F.C., Lican, S., Tolloji, A., Barbieri, P., Tretiach, M., 2015. Seasonal variations of PAHs content and distribution patterns in a mixed land use area: a case study in NE Italy with the transplanted lichen *Pseudevernia furfuracea*. *Atmos. Environ.* 113, 255–263.
- Malaspina, P., Tixi, S., Brunialti, G., Frati, L., Paoli, L., Giordani, P., et al., 2014. Biomonitoring urban air pollution using transplanted lichens: element concentrations across seasons. *Environ. Sci. Pollut. Res.* 21 (22), 12836–12842.
- Murtagh, F., Legendre, P., 2014. Ward's hierarchical agglomerative clustering method: which algorithms implement Ward's criterion? *J. Classif.* 31 (3), 274–295.
- Nieboer, E., Ahmed, H.M., Puckett, K.J., Richardson, D.H.S., 1972. Heavy metal content of lichens in relation to distance from a nickel smelter in Sudbury, Ontario. *Lichenologist* 5 (292304), 45.
- Nimis, P.L., Scheidegger, C., Wolseley, P.A., 2002. *Monitoring With Lichens—Monitoring Lichens*. Kluwer Academic Publishers, Dordrecht NATO Science Series.
- Ocellli, F., Bavdek, R., Deram, A., Hellequin, A.P., Cuny, M.A., Zwarterook, I., Cuny, D., 2016. Using lichen biomonitoring to assess environmental justice at a neighbourhood level in an industrial area of Northern France. *Ecol. Indic.* 60, 781–788.
- Paoli, L., Vannini, A., Monaci, F., Loppi, S., 2018a. Competition between heavy metal ions for binding sites in lichens: implications for biomonitoring studies. *Chemosphere* 199, 655–660.
- Paoli, L., Vannini, A., Fačková, Z., Guarnieri, M., Bačkor, M., Loppi, S., 2018b. One year of transplant: is it enough for lichens to reflect the new atmospheric conditions? *Ecol. Indic.* 88, 495–502.
- Pernigotti, D., Belis, C.A., Spano, L., 2016. SPECIEUROPE: the European data base for PM source profiles. *Atmos. Pollut. Res.* 7 (2), 307–314.
- R Core Team, 2020. *R: A language and Environment For Statistical computing*. R Foundation For Statistical Computing, Vienna (Austria) <https://www.R-project.org/>.
- Ratier, A., Dron, J., Revenko, G., Austruy, A., Dauphin, C.E., Chaspoul, F., Wafo, E., 2018. Characterization of atmospheric emission sources in lichen from metal and organic contaminant patterns. *Environ. Sci. Pollut. Res.* 25 (9), 8364–8376.
- Rola, K., Lenart-Boroń, A., Boroń, P., Osyczka, P., 2020. Heavy-metal pollution induces changes in the genetic composition and anatomical properties of photobionts in pioneer lichens colonising post-industrial habitats. *Sci. Total Environ.* 750, 141439.
- Salameh, D., Detournay, A., Pey, J., Pérez, N., Liguori, F., Saraga, D., et al., 2015. PM<sub>2.5</sub> chemical composition in five European Mediterranean cities: a 1-year study. *Atmos. Res.* 155, 102–117.
- Sylvestre, A., 2016. *Caractérisation de l'aérosol industriel et quantification de sa contribution aux PM 2.5 atmosphériques* (Doctoral dissertation).
- Sylvestre, A., Mizzi, A., Mathiot, S., Masson, F., Jaffrezo, J.L., Dron, J., 2017. Comprehensive chemical characterization of industrial PM<sub>2.5</sub> from steel industry activities. *Atmos. Environ.* 152, 180–190.
- Vannini, A., Guarnieri, M., Paoli, L., Sorbo, S., Basile, A., Loppi, S., 2016. Bioaccumulation, physiological and ultrastructural effects of glyphosate in the lichen *Xanthoria parietina* (L.). *Chemosphere* 164, 233–240.
- Vieira, B.J., Freitas, M.C., Wolterbeek, H.T., 2017. Vitality assessment of exposed lichens along different altitudes. Influence of weather conditions. *Environ. Sci. Pollut. Res.* 24 (13), 11991–11997.
- Zhao, L., Zhang, C., Jia, S., Liu, Q., Chen, Q., Li, X., et al., 2019. Element bioaccumulation in lichens transplanted along two roads: the source and integration time of elements. *Ecol. Indic.* 99, 101–107.
- Zhu, N., Schramm, K.W., Wang, T., Henkelmann, B., Fu, J., Gao, Y., et al., 2015. Lichen, moss and soil in resolving the occurrence of semi-volatile organic compounds on the southeastern Tibetan Plateau, China. *Sci. Total Environ.* 518, 328–336.

## Supplementary materials

### Effects of meteorological conditions and topography on the bioaccumulation of PAHs and metal elements by native lichen (*Xanthoria parietina*)

Julien Dron<sup>1,\*</sup>, Aude Ratier<sup>1,§</sup>, Annabelle Austruy<sup>1</sup>, Gautier Revenko<sup>1</sup>, Florence Chaspoul<sup>2</sup>, Emmanuel Wafo<sup>3</sup>

1. Institut Écocitoyen pour la Connaissance des Pollutions, Fos-sur-Mer, France. E-mail: julien.dron@institut-ecocitoyen.fr
2. Aix Marseille Université, Avignon Université, CNRS, IRD, IMBE, Marseille, France
3. Aix Marseille Université, INSERM, SSA, IRBA, MCT, Marseille, France

-----  
\* Corresponding author. E-mail: julien.dron@institut-ecocitoyen.fr (J. Dron)

§ now at: Univ Lyon, Université Lyon 1, CNRS, LBBE, Villeurbanne, France

## SUPPLEMENTARY MATERIAL S1

Results of quality control measurements (mean values when N>1) for metals (mg.kg<sup>-1</sup>), realized during the different analytical runs of the 2 years of study.

	Al	V	Cr	Mn	Fe	Co	Ni	Cu	Zn	As	Mo	Ag	Cd	Sn	Sb	Hg	Tl	Pb
<b>ERM CD281 RYE GRASS</b>																		
<b>Ref</b>			24.8 *	82 *	180 **		15.2 *	10.2* *	30.5 *	0.04 *	2.22 *		0.12 *	0.06 *	0.04 *	0.02 *		1.67 *
<b>Meas. (N=2)</b>	111	2.51	24.6	77	205	0.10	15.1	10.2	30.7	0.04	2.51	< 0.1	0.12	0.07	0.04	<0.1	<0.1	1.52
<b>IAEA 336 LICHEN</b>																		
<b>Ref</b>	680 **	1.47 **	1.06 **	63 *	430 *	0.29 *		3.6 *	30.4 *	0.63 *			0.12 **		0.07 *	0.2 *		4.9 **
<b>Meas. (N=1)</b>	555	1.51	1.25	63	414	0.25	0,93	3.59	31.0	0.66	0.12	< 0.1	0.10	0.29	< 0.1	0.19	< 0.1	4.69

Results of quality control measurements (mean values when N>1) for PAHs (µg.kg<sup>-1</sup>), realized during the different analytical runs of the 2 years of study.

	Nap	Ace	Acy	Flu	Phe	Ant	FIA	Pyr	BaA	Chr	BbF	BkF	BaP	Dbe	BPe	IPy
<b>Ref. IAEA 451</b>	14.8 *	2 **	2.2	2.6	15.8 *	5.1 **	49.3 *	40 *	19.2 *	26.9 *	35.8 *	14.7 *	18.2 *	5.3 *	19.5 *	23.8 **
<b>Meas. (N=14)</b>	19.7	2.97	3.03	2.24	22.4	2.78	50.9	53.7	20.5	37.2	39.1	16.8	15.3	5.34	17.2	22.4

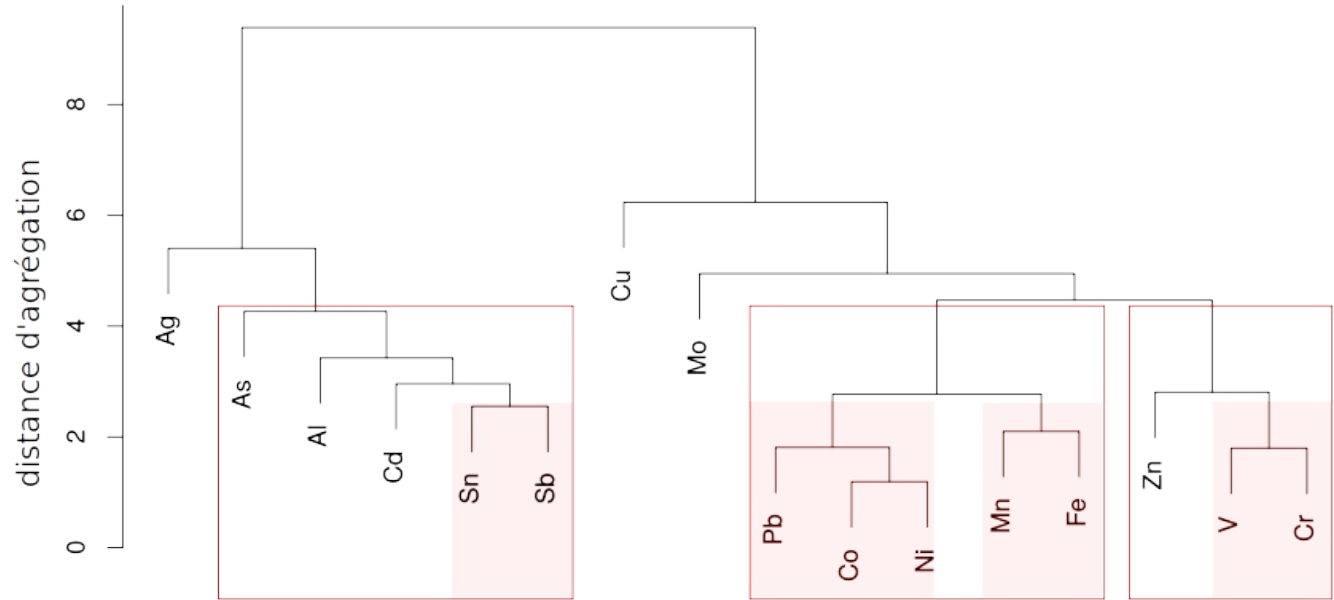
\* certified values

\*\* recommended values

no marker: indicated values

## SUPPLEMENTARY MATERIAL S2

Hierarchical clustering results for metal elements measured in the three investigated sites, during the two years of monitoring (N = 30).





### SUPPLEMENTARY MATERIAL S3

Metal elements concentrations in *X. parietina* along the 2 years of sampling (N = 10 in each site).

	Al	V	Cr	Mn	Fe	Co	Ni	Cu	Zn	As	Mo	Ag	Cd	Sn	Sb	Hg	Tl	Pb
<b>Site i5</b>																		
<b>T1 01/15</b>	5574	15.0	55.0	407	42398	2.06	13.0	20.0	122	4.37	4.14	nd	0.70	9.30	1.79	nd	0.11	39.0
<b>T2 03/15</b>	2694	9.36	30.2	206	17116	1.02	5.77	10.2	53.0	0.90	4.28	0.21	0.22	3.05	0.95	nd	nd	17.8
<b>T3 06/15</b>	2637	9.34	31.7	194	17837	0.96	5.60	9.20	48.0	0.83	3.74	0.22	0.19	2.55	0.77	nd	nd	15.7
<b>T4 09/15</b>	2228	9.60	36.4	245	17286	1.11	6.80	10.8	55.4	1.00	3.64	0.17	0.32	2.66	0.75	nd	nd	15.7
<b>T5 11/15</b>	2192	8.80	29.6	198	14499	0.94	5.70	8.90	43.6	0.83	3.24	0.15	0.28	2.13	0.63	nd	0.15	13.0
<b>T6 01/16</b>	3346	18.6	63.0	291	24341	1.19	6.70	37.0	104	0.98	3.37	0.23	0.30	2.64	0.56	0.20	nd	14.7
<b>T7 03/16</b>	3084	9.80	30.0	230	1821	0.94	5.80	9.00	47.0	0.80	3.06	0.15	0.28	2.06	0.55	nd	0.09	15.1
<b>T8 06/16</b>	1624	6.78	22.0	188	13634	0.75	4.36	8.63	38.2	0.57	1.56	0.12	0.24	2.17	0.53	0.10	nd	15.1
<b>T9 09/16</b>	2447	7.99	27.2	169	14644	0.80	4.19	8.93	56.4	0.59	1.57	0.13	0.39	2.51	0.72	0.11	0.11	13.2
<b>T10 10/16</b>	2924	11.9	34.3	227	18263	1.11	6.30	12.5	86.9	1.55	2.94	0.41	0.49	4.03	1.25	nd	0.10	13.1
<b>Site ui1</b>																		
<b>T1 01/15</b>	3269	8.80	22.0	97.0	4282	1.07	4.50	9.40	60.0	1.82	1.86	nd	0.49	6.20	0.92	nd	nd	14.7
<b>T2 03/15</b>	3143	7.69	21.6	84.0	3929	0.94	4.22	11.2	49.0	0.77	4.17	0.28	0.21	1.75	0.58	2.03	nd	7.70
<b>T3 06/15</b>	2362	5.62	17.6	62.0	2595	0.65	3.00	6.80	44.0	0.61	2.89	nd	0.14	1.27	0.45	0.27	nd	5.50
<b>T4 09/15</b>	1512	4.50	13.7	64.0	2101	0.67	3.10	6.90	39.4	0.68	2.24	nd	0.26	1.18	0.38	nd	nd	5.60
<b>T5 11/15</b>	1708	5.00	15.5	65.0	2278	0.67	3.40	6.80	40.0	0.74	1.92	nd	0.24	1.16	0.39	nd	nd	5.70
<b>T6 01/16</b>	2075	7.40	39.0	85.0	3257	0.68	4.10	21.0	51.0	0.64	2.11	0.19	nd	1.22	nd	0.30	nd	6.20
<b>T7 03/16</b>	2040	5.00	14.0	80.0	3040	0.74	3.20	6.00	38.0	0.62	1.92	0.14	0.22	0.94	0.34	nd	0.03	6.20
<b>T8 06/16</b>	955	3.05	10.0	57.1	2118	0.53	2.12	4.93	25.5	0.44	1.24	nd	0.14	0.84	0.26	0.12	nd	5.23
<b>T9 09/16</b>	1795	5.13	14.8	79.9	3287	0.79	3.22	6.87	32.6	0.61	1.26	nd	0.19	1.19	0.37	0.10	nd	6.72
<b>T10 10/16</b>	1288	6.81	12.6	56.5	2233	0.48	2.11	5.94	14.6	1.80	2.66	0.19	0.06	1.28	0.32	nd	nd	3.66
<b>Site u3</b>																		
<b>T1 01/15</b>	2246	3.30	6.00	44.0	2579	0.79	3.40	9.10	49.0	1.12	0.95	nd	0.26	3.1	0.79	nd	nd	6.10
<b>T2 03/15</b>	2612	5.23	6.20	42.0	2075	0.67	2.81	6.90	26.0	0.51	1.15	nd	nd	1.62	0.54	nd	nd	5.00
<b>T3 06/15</b>	1951	3.96	4.70	30.0	1544	0.49	2.03	6.80	21.0	0.39	0.97	nd	nd	1.26	0.43	nd	nd	3.90
<b>T4 09/15</b>	938	2.90	3.80	30.0	1181	0.52	2.20	6.80	21.6	0.57	0.72	nd	nd	1.17	0.41	nd	nd	3.30
<b>T5 11/15</b>	831	2.30	3.30	23.0	959	0.39	1.90	5.10	17.2	0.47	0.58	nd	nd	0.89	0.30	nd	nd	2.40
<b>T6 01/16</b>	2790	5.20	7.80	48.0	2545	0.66	2.90	26.0	44.0	0.43	2.40	0.74	nd	2.85	1.28	0.45	nd	4.80
<b>T7 03/16</b>	1575	3.13	3.43	29.6	1648	0.49	1.98	5.00	20.1	0.45	1.17	0.08	0.08	0.98	0.37	nd	0.04	3.41
<b>T8 06/16</b>	872	2.07	2.58	23.0	1045	0.36	1.30	4.59	15.8	0.29	0.39	nd	0.06	1.05	0.28	nd	nd	2.63
<b>T9 09/16</b>	1049	2.49	3.22	28.6	1277	0.43	1.65	5.19	18.6	0.36	0.42	nd	0.09	1.17	0.34	nd	nd	3.07
<b>T10 10/16</b>	1744	6.03	5.40	41.5	2115	0.65	2.70	7.59	27.0	1.37	0.84	0.22	0.12	2.17	0.61	nd	nd	4.41

## SUPPLEMENTARY MATERIAL S3 (continued)

PAHs concentrations in *X. parietina* along the 2 years of sampling (N = 10 in each site).

	Nap	Acy	Ace	Flu	Phe	Ant	FlA	Pyr	BaA	Chr	BbF	BkF	BaP	DBA	Bpe	Ipy	HAP <sub>tot</sub>
<b>Site i5</b>																	
<b>T1 01/15</b>	43.2	44.4	124	167	474	12.6	10.2	45.1	16.9	22.4	12.3	7.1	11.0	11.6	9.5	1.3	<b>1013</b>
<b>T2 03/15</b>	55.8	87.8	34.6	26.9	107	74.1	111	42.3	31.1	84.6	58.5	22.2	45.2	40.7	39.7	39.0	<b>901</b>
<b>T3 06/15</b>	78.4	70.1	35.9	32.1	130	125	125	27.2	45.4	113	92.6	29.7	54.2	61.2	70.9	127	<b>1218</b>
<b>T4 09/15</b>	73.9	75.7	90.5	29.7	107	149	118	44.7	35.3	94.6	72.9	35.2	25.7	70.1	36.2	49.4	<b>1108</b>
<b>T5 11/15</b>	69.0	52.0	38.6	22.9	97.9	143	98.8	41.1	29.8	80.9	62.5	20.1	46.9	55.3	38.6	117	<b>1015</b>
<b>T6 01/16</b>	193	21.9	6.40	35.7	352	266	268	403	72.7	159	21.7	25.6	45.2	30.7	60.1	89.6	<b>2051</b>
<b>T7 03/16</b>	175	17.7	9.41	28.4	282	90.4	206	133	44.5	120	82.6	25.7	50.1	15.1	65.9	83.7	<b>1429</b>
<b>T8 06/16</b>	26.7	30.8	13.1	10.9	293	154	227	232	77.6	118	97.1	48.1	75.4	26.1	50.9	58.5	<b>1541</b>
<b>T9 09/16</b>	45.0	33.4	19.7	22.4	273	80.6	207	196	85.1	161	112	73.1	115	40.9	37.4	19.2	<b>1518</b>
<b>T10 10/16</b>	143	12.7	9.74	13.5	209	52.3	148	513	29.2	90.8	80.2	35.9	58.1	57.9	90.9	144	<b>1689</b>
<b>Site ui1</b>																	
<b>T1 01/15</b>	52.5	54.3	303	156	64.8	9.6	13.0	72.5	25.1	6.7	15.1	8.7	7.5	8.8	3.1	0.9	<b>802</b>
<b>T2 03/15</b>	35.5	70.4	39.4	16.9	71.2	204	124	49.2	38.6	86.0	88.6	26.1	82.8	31.1	45.3	104	<b>1114</b>
<b>T3 06/15</b>	53.6	81.2	74.1	18.8	79.9	370	213	51.9	33.7	81.4	82.0	52.4	53.7	89.0	50.2	249	<b>1634</b>
<b>T4 09/15</b>	28.9	41.4	41.3	8.00	47.6	230	98	29.0	27.7	56.0	37.4	17.9	55.1	42.2	41.2	78.4	<b>880</b>
<b>T5 11/15</b>	28.1	57.7	45.2	11.9	45.2	264	107	29.0	32.5	68.4	67.2	26.6	39.5	43.6	38.2	47.3	<b>951</b>
<b>T6 01/16</b>	18.5	9.09	7.99	2.89	175	304	236	344	40.1	80.0	47.6	21.7	37.3	30.6	48.3	94.3	<b>1498</b>
<b>T7 03/16</b>	26.4	7.80	7.96	6.42	167	260	177	93.9	33.4	80.9	73.9	30.0	58.3	8.5	49.0	83.3	<b>1163</b>
<b>T8 06/16</b>	26.3	16.4	9.93	20.6	133	210	180	195	53.2	95.0	78.3	43.5	61.9	5.20	39.3	39.2	<b>1206</b>
<b>T9 09/16</b>	17.7	14.9	13.0	15.4	177	244	235	167	88.2	134	145	67.7	133	18.8	62.8	41.1	<b>1593</b>
<b>T10 10/16</b>	23.0	3.64	5.13	0.02	95.9	111	99.4	565	16.0	29.9	41.0	23.5	87.5	48.2	42.2	47.7	<b>1239</b>
<b>Site u3</b>																	
<b>T1 01/15</b>	22.6	43.8	35.9	14.5	40.6	57.8	57.1	37.8	14.9	45.2	30.3	14.2	19.0	132	22.0	39.4	<b>627</b>
<b>T2 03/15</b>	36.7	53.7	48.0	16.8	55.1	53.0	58.1	39.0	20.0	40.8	24.2	28.2	42.2	184	18.5	71.7	<b>790</b>
<b>T3 06/15</b>	18.2	28.6	33.8	6.79	40.0	72.1	44.2	22.3	9.57	20.5	19.2	7.2	16.2	51.2	13.0	23.7	<b>427</b>
<b>T4 09/15</b>	24.5	20.4	46.5	7.44	30.5	61.9	38.9	22.8	6.08	18.4	21.2	12.1	27.9	30.0	15.6	37.5	<b>422</b>
<b>T5 11/15</b>	25.8	32.9	44.4	10.4	34.9	67.2	45.0	22.7	3.93	22.6	16.7	13.0	31.4	58.5	7.73	94.3	<b>531</b>
<b>T6 01/16</b>	30.5	3.03	3.26	3.33	93.6	73.1	88.4	166	8.34	27.1	12.3	5.7	7.01	40.2	28.1	43.2	<b>633</b>
<b>T7 03/16</b>	13.2	3.53	4.88	5.44	95.0	45.9	77.3	28.8	6.91	22.9	6.14	12.5	16.7	5.87	14.1	4.45	<b>364</b>
<b>T8 06/16</b>	25.7	11.4	7.08	7.21	87.0	51.2	86.9	119	19.4	30.2	28.4	20.2	27.0	9.96	14.4	6.12	<b>551</b>
<b>T9 09/16</b>	26.8	9.06	6.34	7.61	70.3	44.9	72.4	101	14.5	31.1	23.1	20.5	24.5	2.08	10.8	9.73	<b>475</b>
<b>T10 10/16</b>	15.2	4.04	4.55	1.36	70.1	25.9	62.7	290	1.97	14.6	16.0	16.1	62.1	12.2	29.0	34.9	<b>661</b>

### SUPPLEMENTARY MATERIAL S4

Evolution of PM10 levels (seasonal averages,  $\mu\text{g}\cdot\text{m}^{-3}$ ), in three monitoring stations of in the study are (see Figure 1 for approximate locations). Data obtained from AtmoSud (2020).

